J. Biochem. **134**, 575–581 (2003)
DOI: 10.1093/jb/mvg176

More Ordered, Convex Ganglioside-Enriched Membrane Domains: The Effects of GM_1 on Sphingomyelin Bilayers Containing a Low Level of Cholesterol

Bo Pei and Jian-Wen Chen*
National Laboratory of Biomacromolecules, Institute of Biophysics, Academia Sinica, Beijing 100101, China

Received June 18, 2003; accepted August 1, 2003

The special physical state of the sphingolipid-enriched membranes with characteristic lipid composition, presently one of the most controversial foci in cell biology, provides the essential environment for the proteins inside to be involved in the related physiological processes. The role of gangliosides, an important component of the membranes, deserves attention. The present investigation using several biophysical techniques indicates that ganglioside GM_1 induces the phase separation in the sphingomyelin membrane with 5 mol% cholesterol and regulates the membrane structure. The results of differential scanning calorimetry show that a higher T_m, GM_1-rich phase emerges behind the lower T_m, sphingomyelin-rich phase with the incorporation of GM_1 into the sphingomyelin/cholesterol bilayers; and the GM_1-rich phase dominates the membrane when the proportion of GM_1 reaches about 20 mol%. Fluorescence quenching further shows that the separation of the two domains is independent of temperature, occurring both in the gel phase and in the liquid phase. Laser Raman spectroscopy and fluorescence polarization suggest that the order of hydrocarbon chains increases and membrane fluidity decreases with increase in GM_1 content. Use of the fluorescence probe merocyanine-540 and electron microscopy reveals that the insertion of GM_1 leads to an increase in the spatial density of the lipid headgroups and a decrease in the curvature of the sphingomyelin/cholesterol bilayers. In sums, both the hydrophilic sugar heads and the hydrophobic hydrocarbon chains of GM_1 contribute to the regulation of membrane architecture. We suggest that the convex curvature of ganglioside-enriched membrane could be involved in forming and maintaining the characteristic flask-shaped invagination of caveolae.

Key words: ganglioside GM_1, membrane domains, membrane structure, phase separation, sphingomyelin/cholesterol bilayer membrane.

Abbreviations: 3-AS, 3-(9-anthroyloxyl)-stearic acid; 5-DS, 5-doxyl stearic acid; 16-AP, 16-(9-anthroyloxyl)-palmitic acid; Chol, cholesterol; DIM, detergent-insoluble membrane; DPH-PC, 2-(3-(diphenylhexatrienyl)-propanoyl)-1-hexadecanoyl-*sn*-glycero-3-phosphocholine; DSC, differential scanning calorimetry; GEMs, glycosphingolipid-enriched membrane domains; GSDs, glycosphingolipid signaling domains; MC-540, merocyanine-540; SPM, sphingomyelin.

A remarkable inherent property of glycosphingolipids (especially gangliosides) is their ability to interact with each other to form microclusters at the cell surface (*1*). In the last few years, glycosphingolipid-enriched membrane domains (GEMs) have been proved to selectively concentrate some proteins and to be involved in signal transduction, in which glycosphingolipids act as the receptors and are coupled with the transducers (*2*, *3*). GEMs are not equal to caveolae, which have a characteristic flask-shape structure, although they are both Triton X-100 insoluble at low temperature and have a light buoyant density. Hakomori and co-workers have immunoprecipitated GEMs and caveolin-rich membranes from detergent-insoluble membranes, and proved that the two fractions have different composition and functions (*3*). GEMs contain gangliosides, sphingomyelin but only low amount of cholesterol, while caveolin-rich membranes are cholesterol-dependent and deficient in sphingolipids; GEMs are devoid of caveolin but are enriched in Src, FAK and Rho A, so they are involved in glycosphingolipid-dependent cell adhesion coupled with signal transduction, while caveolin-rich membranes are deficient in these proteins and depletion of cholesterol has no effect on the signaling (*3*, *4*). Biochemical and microscopic studies by Sonnino's group also showed that caveolin and ganglioside-enriched domains had different distributions (*5*). It has been suggested that the glycosphingolipid-enriched membrane is a structural and functional unit and as such it has been named glycosphingolipid signaling domain (*2*, *3*).

Gangliosides, sialic acid-containing glycosphingolipids, have a ceramide backbone and very complex sugar headgroups, which makes their contribution to membrane architecture unique (*6*, *7*). It has been proved that ganglioside GM_1 was incorporated gradually into DPPC bilayers at lower contents and reduced their transition enthalpy; when GM_1 content was higher than 30 mol%, GM_1 promoted DPPC bilayers to collapse to micelle (*8*). Masserini's group found that for a given oligosaccharide

*To whom correspondence should be addressed. Tel: +86-10-64888523, Fax: +86-10-64872026, E-mail: chenmaci@sun5.ibp.ac.cn

composition, gangliosides exhibited lateral phase separation to an extent dependent on the length and unsaturation difference between ganglioside long-chain base and phosphatidylcholine acyl chain; for a given ganglioside lipidic composition, the extent of phase separation was dependent on the number of sugar units present in the glycolipid (*9*, *10*). In another paper, they reported that the architectural features of sphingomyelin bilayers were strongly dependent on the presence of ganglioside GM_1, which leads to formation of separate, GM_1-enriched domains (*11*). Up to now, however, the physical state of glycosphingolipid-enriched membranes and the effects of gangliosides on the sphingomyelin bilayers containing a low level of cholesterol have not been explored in detail, even though such an investigation would be helpful to understand the function of gangliosides in the glycosphingolipid-enriched domains and the roles of these domains under physiological conditions.

In this paper, we report a study performed with a combination of different biophysical methods aimed to obtain information about the effects of ganglioside GM_1 on the SPM/Chol bilayer membrane. Using the differential scanning calorimetry (DSC) and fluorescence quenching, we confirmed that GM_1 can induce the appearance of a GM_1-enriched phase in the SPM/Chol membrane. Changes of membrane fluidity were studied by laser Raman spectroscopy and fluorescence polarization, both of which indicated that membrane fluidity decreases gradually with increase in GM_1 content. The head region of the bilayers was examined with MC-540, and the results showed that the spatial density of headgroups decreases because of insertion of the large, net negatively charged sugar chains of GM_1. Furthermore, membrane curvature was shown to increase by electron microscopy, as expected.

MATERIALS AND METHODS

Materials—3-AS, 16-AP, 5-DS, DPH-PC, and MC-540 were purchased from Molecular Probes. Sphingomyelin (chicken egg yolk), cholesterol and GM_1 (bovine brain) were from Sigma Chemical (St. Louis, MO). All other chemicals were of analytical grade.

Samples—Lipid mixtures of various molar ratios were made into thin films by dissolving lipids in a small volume of chloroform/methanol (4:1, v/v), evaporating the solvent under a stream of nitrogen, and vacuumizing for over 3 h. Large multilamellar liposomes were subsequently prepared by suspending the dried lipids in 20 mM Tris-HCl, 150 mM KCl (pH 7.5) buffer (for the most experiments) and PBS buffer (pH 7.4 for laser Raman experiments), and vortexing vigorously for 10 min at 50°C.

Small unilamellar liposomes were prepared by intermittent probe sonication of the suspension of large multilamellar liposomes in CPX 600 ultrasonic homogenizer (Cole-Parmer) at 4°C. Sonication was performed for 4 min and the power was 120 W.

The GM_1 contents were calculated by

$$GM_1\ (\text{mol}\%) = GM_1/(\text{SPM} + GM_1).$$

The Chol content was constant in all samples and was calculated by

$$\text{Chol}\ (\text{mol}\%) = \text{Chol/SPM} = 5\ \text{mol}\%.$$

Differential Scanning Calorimetry—Samples were run on a high sensitivity MC-2 differential scanning calorimeter interfaced to an IBM microcomputer (Microcal, Northampton, MA). The samples were carefully degassed before the calorimetric scans were performed. Each sample was scanned at a rate of 60°C/h. The temperature of maximum heat absorption was defined as the phase-transition temperature (T_m), the transition enthalpy (ΔH) was calculated from the area under the endothermic peak using the software subroutines provided by Microcal, and the curve-fitting was finished in Origin 6.1.

Fluorescence Quenching—All the samples had the DPH-PC: $\text{lipids}_{\text{total}}$ = 1:500 (molar ratio), and the molar ratios of quencher, 5-DS, to total lipids were 0, 0.02, 0.04, 0.08, and 0.16. All fluorescence spectra were recorded on a Hitachi F-4010 fluorescence spectrophotometer at 30°C and 50°C. The excitation wavelength was 350 nm and the emission intensity at 430 nm was recorded. The ratios of the fluorescence emission intensity of the samples (F) and that of samples without quencher (F_0) were used to show the extent of quenching.

Laser Raman Spectroscopy—The samples were spread on a quartz slide and covered with a cover glass. The samples were focused with a microscope produced by Olympus. Raman spectroscopy was performed on a JY-T64000 Raman spectrophotometer fitted with a NIC-1180 computer and an argon-ion laser Model 164 produced by Spectra Physics, USA. The 514.5 nm line was used as irradiation for the photosensitization and excitation of the samples. The experimental conditions were as follows: the exciting line was 514.5 nm and the power was 500 mW; the widths of both slits of the monochromators were 300 μm; scanning ranges were 600–1,800 cm^{-1} and 2,800–3,000 cm^{-1}; the spectra were accumulated for 30 times for each sample; the room temperature at that time was 18°C. The control spectrum of PBS buffer (pH 7.4) was deducted when the data were processed with the software Origin 6.1.

The order parameter for the lateral interaction between chains (S_{lat}) was calculated by

$$S_{\text{lat}} = (I_{2890}/I_{2850} - 0.7)/1.5$$

and the longitudinal order parameter in chains (S_{trans}) was calculated by

$$S_{\text{trans}} = (I_{1130}/I_{1090})/1.77 \qquad (12, 13).$$

Fluorescence Polarization—The fluorescence probes and the lipids were mixed at a probe-to-lipid molar ratio of 1:400, followed by preparation of large multilamellar liposomes and incubation at 50°C for 1 h. Fluorescence measurements were performed on a Hitachi F-4010 fluorescence spectrophotometer with a thermostat. The excitation wavelength and the emission wavelength were 388 nm and 455 nm, respectively. The polarization degree (P) was calculated according to the following formula:

$$P = (I_{VV} - G \cdot I_{VH})/(I_{VV} + G \cdot I_{VH}) \quad (14).$$

MC-540 Fluorescence—MC-540 was added to large multilamellar liposomes at a probe-to-lipid molar ratio of 1:200. The excitation wavelength was 540 nm and the emission intensity at 590 nm was recorded.

Transmission Electron microscopy—Droplets of 5 μl of liposomes were applied to copper grids coated with carbon film previously rendered hydrophilic by glow discharge in air. The excess samples were removed after 60 s by blotting with filter paper and negatively stained with 1% aqueous uranyl acetate for 2 min, blotted, and dried in air. Micrographs of the negatively stained liposomes were recorded in a TECNAI 20 (Philips) transmission electron microscope at 50,000× magnification, which was operated at 120 kV.

RESULTS

Differential Scanning Calorimetry—The thermotropic behavior of SPM liposomes containing 5% mol Chol and increasing GM_1 contents were compared by differential scanning calorimetry. Figure 1 shows that the DSC thermograms are fitted by two components. With the increase in the proportion of GM_1 in the liposomes, the main, sharper, lower temperature (39.1°C) melting component decreases in amplitude and finally disappears; and at the same time, the minor, broader, higher temperature (42.5°C) melting component, undetectable in the absence of GM_1, increases in amplitude and becomes the principal part. These results suggest that the lower temperature peak is related to the domains mainly composed of SPM, while the higher temperature peak is to a phase-separated, ganglioside-rich domain.

Fluorescence Quenching—The quenching of DPH fluorescence by the doxyl groups in mixtures of SPM/Chol with increasing GM_1 contents is shown in Fig. 2, A and B, for data obtained at 30°C and 50°C, respectively. The most obvious quenching of DPH fluorescence occurs in the SPM/Chol bilayer without GM_1. The increase of GM_1 proportion to 10 mol% leads to progressively less quenching, but the further incorporation of GM_1 to 20 mol% conversely potentiates the quenching of DPH fluorescence. The most quenching should occur in a single-phase, homogeneous system because this provides the most favorable environment for fluorophores and quenchers to make frequent contact. When the single phase separates, closed and unconnected microdomains are formed over the whole bilayer, and the heterogeneous distribution of fluorophores and quenchers in such microdomains leads to the decline of effective quenching (*15*). In our experiments, the bilayer membrane is either in the liquid phase or in the gel phase at the temperatures employed, that is, it should be a single phase, but the results indeed show that it becomes heterogeneous and there exist different domains in the bilayers with about 5–10 mol% GM_1 in liposomes. This is understandable in the light of the DSC results that GM_1 promotes the appearance of a ganglioside-rich phase that coexists with the original SPM-rich phase. These results indicate, regardless of temperature, gangliosides induce the appearance of a new domain that finally extends over the whole membrane.

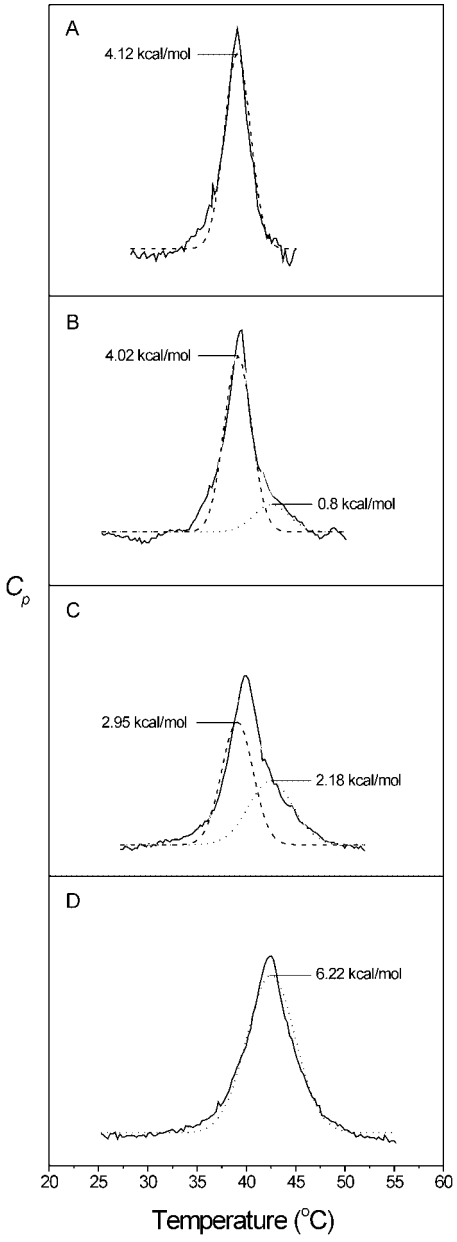

Fig. 1. **C_p *vs* temperature plot of the SPM/Chol liposomes containing different proportions of GM_1 (solid lines) and illustrations of the curve-fitting procedure used to resolve the components of the DSC thermograms exhibited by the SPM/Chol liposomes with increasing GM_1 proportions (dotted lines).** The enthalpies of the components are showed by the corresponding transition peaks. (A) 0 mol% GM_1, (B) 5 mol% GM_1, (C) 10 mol% GM_1, (D) 20 mol% GM_1.

Laser Raman Spectroscopy—The dynamic growth and disappearance of the domains in the SPM/Chol/GM_1 bilayers must lead to changes in the physical state of the membrane. Here, laser Raman spectroscopy and fluorescence polarization were employed to reflect membrane fluidity, which is an important physical parameter describing the hydrophobic region of the membrane. Raman lines were observed in the regions 1,000–1,300

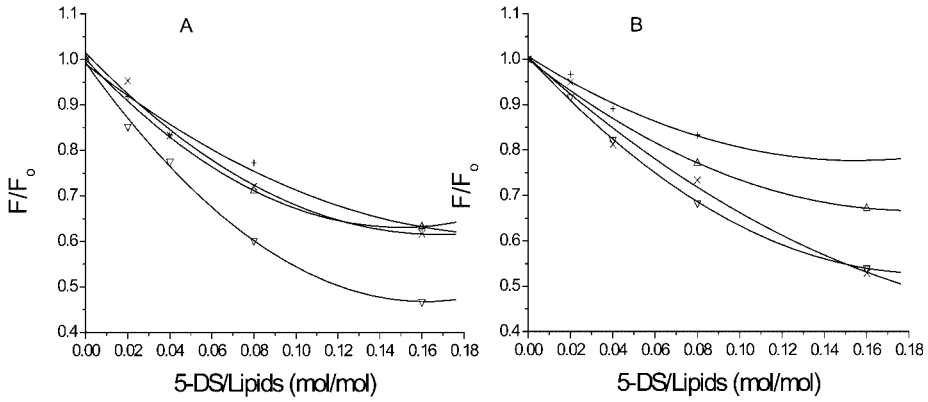

Fig. 2. **Fluorescence quenching of DPH-PC by 5-DS (F/F_0) was assayed at 30°C (A) and 50°C (B) in the SPM/Chol liposomes with different GM_1 contents.** (inverted triangles) 0 mol% GM_1, (triangles) 5 mol% GM_1, (+) 10 mol% GM_1, (×) 20 mol% GM_1. The concentration of SPM was 0.1 mM for all samples.

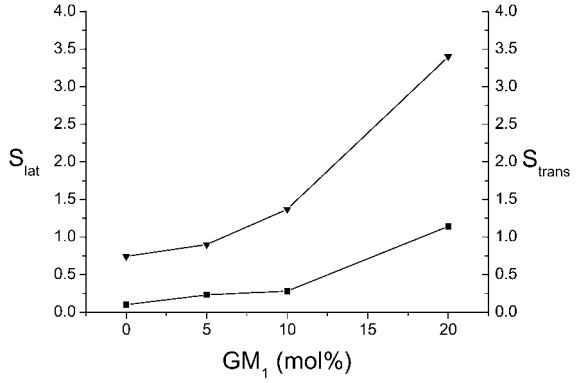

Fig. 3. **The order parameter for the lateral interaction between chains (S_{lat}, squares) and the longitudinal order parameter in chains (S_{trans}, inverted triangles) were assayed as functions of the GM_1 contents by laser Raman spectroscopy at 18°C.** The lipid concentration was 10% (w/v) for all samples.

cm^{-1} and 2,800–3,000 cm^{-1}. The former is that of the C–C stretching vibration, and the latter that of the C–H stretching vibration, both of which are very sensitive to membrane structure (*12*, *13*). The lateral interaction order-parameter between chains (S_{lat}) and the longitudinal order-parameter in chains (S_{trans}) *vs.* the GM_1 proportion in the SPM/Chol liposomes are plotted in Fig. 3.

Two bands, $-CH_2-$ symmetric (2,850 cm^{-1}) and asymmetric (2,890 cm^{-1}) stretching vibrations, are used widely to study the conformation of hydrocarbon chains. S_{lat}, calculated from I_{2890}/I_{2850}, reflects the lateral packing of hydrocarbon chains (*12*, *13*, *16*). Figure 3 shows a monotonic increase of the order parameter with increasing GM_1 content in the SPM/Chol bilayers. From this it can be inferred that GM_1 makes the hydrocarbon chains in the SPM/Chol membrane pack more tightly.

The bands at 1,130 cm^{-1} and 1,190 cm^{-1} are assigned to the vibration mode of all-*trans* chain segments and *gauche* rotamers, respectively. The more all-*trans* bonds appear, the higher the longitudinal order-parameters are, while the opposite is true for *gauche* rotamers. Therefore, the ratio of the band intensity at 1,130 cm^{-1} and 1,190 cm^{-1}, I_{1130}/I_{1190}, is relevant to the longitudinal order degree of hydrocarbon chains (*12*, *13*, *16*). From Fig. 3, it can be seen that S_{trans}, developed from I_{1130}/I_{1190}, increases progressively with GM_1 incorporation into the SPM/Chol bilayers, indicating that the *trans* conformers of hydrocarbon chains increase while the *gauche* rotamers decrease, that is, GM_1 induces higher ordering of the hydrocarbon chains.

The above results indicate that the incorporation of GM_1 constrains the mobility of hydrocarbon chains in the bilayers in both the lateral and longitudinal directions.

Fluorescence Polarization—Unlike laser Raman, n-AS and 16-AP can show fluidity of a certain region of the membrane by their 9-anthroyloxy fluorescent groups at different positions of the acyl chains (*17*). Figure 4 reveals that whether in the gel phase or in the liquid phase, in the head region (Fig. 4A) or in the hydrophobic-core region (Fig. 4B), the fluorescence polarization increases progressively with GM_1 incorporation into the SPM/Chol liposomes. This indicates that GM_1 reduces

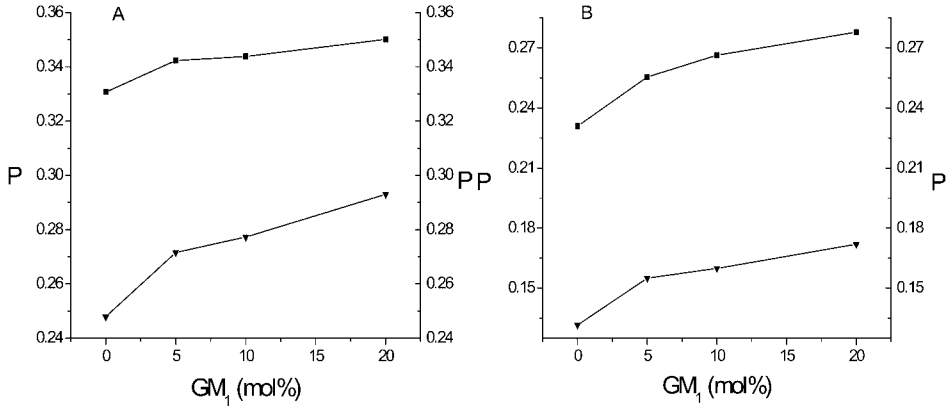

Fig. 4. **Fluorescence polarization of 3-AS (A) and 16-AP (B) were assayed as the functions of the GM_1 contents at 30°C (squares) and 50°C (inverted triangles).**

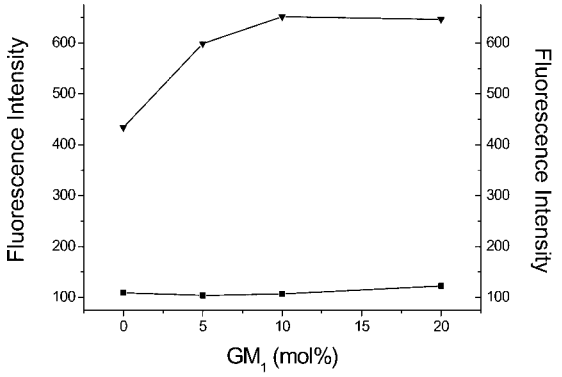

Fig. 5. **The fluorescence intensity of MC-540 was assayed as a function of the GM_1 contents at 30°C (squares) and 50°C (inverted triangles).** The concentration of SPM was 0.1 mM for all samples.

membrane fluidity in a content-dependent manner in all regions of the bilayers.

MC-540 Fluorescence Intensity—MC-540 has successfully been used as an optimal probe to detect the degree of headgroup spacing of lipid bilayers. From aqueous to non-aqueous solvents, the maximal fluorescence emission peak of MC-540 shifts from 570 nm to 590 nm, accompanied by a large increase in the fluorescence yield (*18*). As illustrated in Fig. 5, in the gel phase, no obvious increase in fluorescence intensity of MC-540 is observed with increasing GM_1 content, which indicates that GM_1 has very weak effect in reducing the spatial density of lipid headgroups at lower temperature. However, in the liquid phase, GM_1 clearly promotes the enhancement of fluorescence intensity, that is, the distance between lipids in the head region of the bilayer is effectively increased.

Electron Microscopy of Negatively Stained Small Unilamellar Liposomes—Membrane curvature is another important physical parameter, which is in inverse proportion to the radii of the lipid vesicles. The above results have indicated that, on the one hand, GM_1 makes the hydrocarbon chains pack more tightly; on the other hand, the distance between lipid headgroups increases with the insertion of GM_1 into the bilayers. So a lipid molecule in the outer layer probably occupies an inverse cone-shaped space, and the layer should accordingly have a positive curvature. The observation of small unilamellar liposomes with different GM_1 contents by electron microscopy confirms this supposition (Fig. 6). With increasing GM_1 incorporation into the bilayers, the liposomes become smaller and smaller. The statistical results of the vesicle diameters are listed in Table 1, from which it can be inferred that GM_1 plays an important role in regulating membrane curvature.

Table 1. **Diameters of the SPM/Chol small unilamellar vesicles containing 0, 10, or 20 mol% GM_1.**

GM_1 content in the liposomes	0 mol%	10 mol%	20 mol%
Diameters of the liposomes	238 nm[a]	209 nm[b]	130 nm[c]

[a]$p < 0.01$, $n > 20$, [b]$p < 0.05$, $n > 20$, [c]$p < 0.01$, $n > 20$.

DISCUSSION

Gangliosides, which have hydrophobic ceramide backbones and hydrophilic sugar heads, interact with other membrane lipids so that the architectural features of lipid bilayers are strongly dependent on them (*8–11*). The finding of sphingolipid-enriched domains supports this point of view and provides more clues to understand the dynamics of glycosphingolipids in the plasma membrane. The goal of this investigation is to determine the effects of gangliosides on the sphingomyelin bilayers containing a low level of cholesterol in detail and try to gain deeper insights into the nature of glycosphingolipid-enriched membrane domains (GEMs). The results obtained indicate that with increase in its concentration, GM_1 induces phase separation, a GM_1-rich phase coexisting with a SPM-rich phase; and at 20 mol% GM_1, the former becomes dominant in the membrane. In fact, regardless of temperature, these two domains separate both below T_m and above T_m (Fig. 2). With the formation and growth of the GM_1-rich domains, the physical state of the lipid bilayers changes accordingly. Membrane fluidity gradually decreases with increase in GM_1 content, and hydrocarbon chains become more extended and pack more tightly. The insertion of GM_1 with the large, net negatively charged sugar heads in the bilayers increases membrane curvature and "loosens" the head region of the bilayers.

The concept that more hydrogen bonds exist among sphingolipids than phosphoglycerides has been accepted

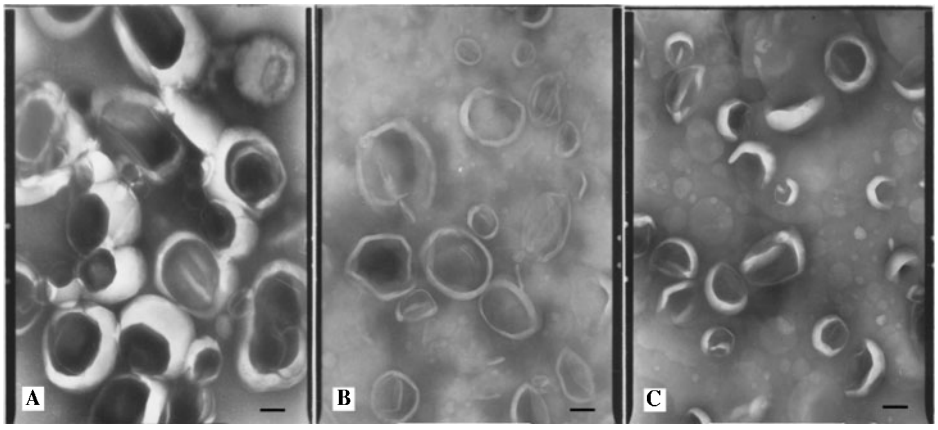

Fig. 6. **Micrographs of SPM/Chol small unilamellar liposomes with different GM_1 contents.** The lipid concentration was 1 mg/ml for all samples. (A) GM_1 (mol%) = 0, (B) GM_1 (mol%) = 10, (C) GM_1 (mol%) = 20. Scale bars, 100 nm.

widely, and this is suggested to be one of factors that drives the former to separate from the latter environment in the plasma membrane (*7*, *19*, *20*). However, compared with sphingomyelin, glycosphingolipids are much more capable of forming hydrogen bonds with their complex sugar chains. Ferraretto and co-workers suggested that the potent tendency of gangliosides to self-associate, possibly through carbohydrate-carbohydrate interaction, could lead to the formation of a ganglioside-enriched, GM_1/SPM-mixed domains separated from the SPM bilayers (*11*). On the other hand, the hydrocarbon chains of gangliosides also contribute to the phase separation in the membrane. Segregation of GM_1 from DMPC bilayers but homogeneity in GM_1/DPPC bilayers showed the main driving force for ganglioside lateral phase separation in ganglioside/phospholipid bilayers to be a difference in the chain length of the glycolipid and of the phospholipid bilayer matrix (*9*, *10*). In fact, the presence of long and saturated hydrocarbon chains is another factor promoting the separation of the sphingolipid domains from the phosphoglyceride environment (*7*, *19*, *20*). Generally, glycosphingolipids, especially from brains, have longer hydrocarbon chains than sphingomyelin (*6*, *21*, *22*). So, to sum up, phase separation and fusion of the ternary SPM/Chol/GM_1 mixture depend on both the headgroups and the hydrocarbon chains. It should be pointed out that in our experiments, different from that of Ferraretto et al., no Chol-enriched phase is observed, which is probably because the sphingomyelin used here is mixed-chain (chicken egg yolk) rather than palmitoylsphingomyelin (*11*). Since it has been proved that the Chol-enriched phase was constant both in its T_m and its ΔH in the experimental range, our use of mixed-chain sphingomyelin will have no effects on the above conclusion. Fluorescence quenching is a highly sensitive method to examine the phase separation in lipid bilayers, which does not require a large difference in the physical properties of the two phases (*23*). The result obtained here that the process of separation and fusion of the domains in the SPM/Chol/GM_1 bilayers occurs both in the gel phase and in the liquid phase indicates that temperature has no evident effect on the interactions among the three lipids.

The insertion of gangliosides into lipid bilayers usually leads to the decrease of membrane fluidity. This can be understood as a result of their long and saturated fatty acyl chains and the fact that they induce the formation of many hydrogen bonds. It was reported that a PC bilayer membrane containing 18-carbon fatty acid glycosphingolipids was much more fluid than one containing a 24-carbon fatty acid analogue (*24*). In this investigation, compared with sphingomyelin from egg yolk, gangliosides from brain have longer sphingoid bases and fatty acyl chains (*6*, *25*, *26*). The longer hydrocarbon chain contributes to the higher transition temperature, which means that there exist more *trans* conformers and less *gauche* rotamers in the longer chains than in the short chains at a certain temperature, that is, the former are more extended and can pack more tightly in the membrane. On the other hand, the abundance of hydrogen bond acceptors and donors provided by gangliosides promote the formation of a hydrogen bond network among gangliosides and other lipids, which stabilizes the membrane and, at the same time, constrains the motility of these lipids. As a result, membrane fluidity decreases. Moreover, the decrease occurs in both the head region and the hydrophobic-core region, as indicated in Fig. 4.

At the water/lipid interface, the individual ganglioside molecules occupy a large surface area due to their net negatively charged, bulky oligosaccharide chains (*27*), which leads ganglioside-enriched domains to display a membrane geometry characterized by a partially convex curvature (*28*). Except for GM_3, which self-assembles in vesicles, other gangliosides with the headgroups of increasing complexity and extension are cone-shaped and tend to form micelle (*29*). When GM_1 content was more than 30 mol% in the DPPC bilayers, a micella phase appeared in the calorimetric thermograms; and more than 60 mol%, GM_1 induced the whole DPPC bilayer to be converted to micelle (*8*). Consistent with the above conclusions, our results from electron microscopy prove that the incorporation of GM_1 into the lipid bilayers leads to an increase in membrane curvature. Meanwhile, the determination of the spatial packing of lipid headgroups here also shows that the distance between lipid headgroups gradually increases as GM_1 content increases from 0 to 20 mol%. But due to the tighter packing in the gel phase than the liquid phase, the increase in distance between headgroups is much less obvious in the gel phase than the liquid phase (Fig. 5). It should be pointed out that GM_1 does not really "loosen" the head region, considering the more and more tightly packing hydrocarbon chains, that is, the increasing distance between headgroups is passive because of strong repulsion attributed mainly to steric hindrance and partly to electrostatic forces (*29*).

Lipids are distributed not only asymmetrically between the two layers of biomembranes, but also inhomogeneously within a layer. In recent years, sphingolipid-enriched membrane domains have been found and have become a focus of today's biology. Sphingolipid-rich membranes are usually highly enriched in cholesterol. However, ganglioside-enriched and cholesterol-deficient membrane domains have been proved to exist under physiological conditions (*3*, *5*) and were primarily explored in *in vitro* experiments (*11*). We suggest that the special physical state of the ganglioside-enriched membrane domains with a low level of cholesterol could provide the optimal environment for certain proteins to reside and/or function. Each domain could be a functional unit, and when the cell is stimulated, these "floating" membrane domains on the plasma membrane could associate with each other, or even with other membrane domains, to be involved in the relevant physiological processes. On the other hand, their special architectural characteristics make them function as a structural unit. Chigorno *et al*. pointed out that the flask-shaped invagination of caveolae was not an ideal place for micella-forming gangliosides (*5*). They suggested that ganglioside clusters could reside at the edges of the invagination, where membrane domains with convex curvature were available. Supporting the above hypothesis, our results from electron microscopy and MC-540 provide direct proofs *in vitro* that the ganglioside-enriched and cholesterol-deficient domains have the convex membrane curvature. Obviously, the appearance of a high content of cholesterol in the outer plasma membrane layer of these

regions is improper, because cholesterol could promote an increased curvature radius by filling the voids between lipid molecules (*29*); on the contrary, the outer membrane layer in caveolar cavity, which is concave, could contain a high amount of cholesterol but a low amount of glycosphingolipids. We suggest that the caveola membrane is inhomogeneous, and glycosphingolipids and cholesterol function as effectors to regulate the architecture of different membrane regions; the ganglioside-enriched but cholesterol-deficient membrane domains could be located at the edges of an invagination and, together with some certain functional proteins (*30*), contribute to forming and maintaining the characteristic structure of caveolae.

We were very grateful to Prof. Yi-Ming Xu for her advice about laser Raman spectroscopy. This work was supported by the National Nature Science Foundation of China (30070186 and 30230120) and National Laboratory of Biomacromolecules (881613).

REFERENCES

1. Rock, P., Allietta, M., Young, W.W.J., Thompson, T.E., and Tillack, T.W. (1990) Organization of glycosphingolipids in phosphatidylcholine bilayers, use of antibody molecules and Fab Fragments as morphologic markers. *Biochemistry* **29**, 8484–8490
2. Yamamura, S., Handa, K., and Hakomori, S.-I. (1997) A close association of GM_3 with c-Src and Rho in GM_3-enriched microdomains at the B16 melanoma cell surface membrane, a preliminary note. *Biochem. Biophys. Res. Commun.* **236**, 218–222
3. Iwabuchi, K., Handa, K., and Hakomori, S.-I. (1998) Separation of "glycosphingolipid signaling domain" from caveolin-containing membrane fraction in mouse melanoma B16 cell and its role in cell adhesion coupled with signaling. *J. Biol. Chem.* **273**, 33766–33773
4. Hakomori, S.-I., Handa, K., Iwabuchi, K., Yamamura, S., and Prinetti, A. (1998) New insights in glycosphingolipid function, "glycosignaling domain, " a cell surface assembly of glycosphingolipids with signal transducer molecules, involved in cell adhesion coupled with signaling. *Glycobiology* **8**, xi–xix
5. Chigorno, V., Palestini, P., Sciannamblo, M., Dolo, V., Pavan, A., Tettamanti, G., and Sonnino, S. (2000) Evidence that ganglioside enriched domains are distinct from caveolae in MDCK II and human fibroblast cells in culture. *Eur. J. Biochem.* **267**, 4187–4197
6. Ledeen, R.W. and Yu, R.K. (1982) Gangliosides, structure, isolation, and analysis. *Methods Enzymol.* **83**, 139–191
7. Brown, R.E. (1998) Sphingolipid organization in biomembranes, what physical studies of model membranes reveal. *J. Cell Sci.* **111**, 1–9
8. Reed, R.A. and Shipley, G.G. (1996) Properties of ganglioside GM_1 in phosphatidylcholine bilayer membranes. *Biophysical J.* **70**, 1363–1372
9. Masserini, M., Palestini, P., and Freire, E. (1989) Influence of glycolipid oligosaccharide and long-chain base composition on the thermotropic properties of dipalmitoylphosphatidylcholine large unilamellar vesicles containing gangliosides. *Biochemistry* **28**, 5029–5034
10. Terzaghi, A., Tettamanti, G., and Masserini, M. (1993) Interaction of glycosphingolipids and glycoproteins, thermotropic properties of model membranes containing GM_1 ganglioside and glycophorin. *Biochemistry* **32**, 9722–9725
11. Ferraretto, A., Pitto, M., Palestini, P., and Masserini, M. (1997) Lipid domains in the membrane, thermotropic properties of sphingomyelin vesicles containing GM_1 ganglioside and cholesterol. *Biochemistry.* **36**, 9232–9236
12. Gaber, B.P. and Peticolas, W.L. (1977) On the quantitative interpretation of biomembrane structure by Raman spectroscopy. *Biochim. Biophys. Acta* **465**, 260–274
13. Tu, A.T. (1982) *Raman Spectroscopy in Biology*, *Principles and Applications*, pp. 187–233, John Wiley & Sons, New York
14. Wang, P.-Y., Chen, J.-W., and Hwang, F. (1993) Anisodamine causes acyl chain interdigitation in phosphatidylglycerol. *FEBS Lett.* **332**, 193–196
15. Piknova, B., Marsh, D., and Thompson, T.E. (1996) Fluorescence-quenching study of percolation and compartmentalization in two-phase lipid bilayers. *Biophysical J.* **71**, 892–897
16. Xu, Y.-M., Zhang, Z.-Y., and Zhang, W. (1998) Raman spectroscopic characteristics of microcosmic and photosensitive damage on space structure of liposomes sensitized by hypocrellin and its derivatives. *Sci. China C* **41**, 459–464
17. Zhang, Z.-G., Lu, J.-Z., and Chen, J.-W. (1999) Concanavalin A binding to oligosaccharide chain leads to alterations in properties of Band 3. *Biochem. Mol. Biol. Int.* **47**, 377–385
18. Williamson, P., Mattocks, K., and Schlegel, R.A. (1983) Merocyanine-540, a fluorescent probe sensitive to lipid packing. *Biochim. Biophys. Acta* **732**, 387–393
19. Brown, D.A. and London, E. (2000) Structure and function of sphingolipid- and cholesterol-rich membrane rafts. *J. Biol. Chem.* **275**, 17221–17224
20. Rietveld, A. and Simons, K. (1998) The differential miscibility of lipids as the basis for the formation of functional membrane rafts. *Biochim. Biophys. Acta* **1376**, 467–479
21. Barenholz, Y. and Thompson, T.E. (1980) Sphingomyelins in bilayers and biological membranes. *Biochim. Biophys. Acta* **604**, 129–158
22. Thompson, T.E. and Tillack, T.W. (1985) Organization of glycosphingolipids in bilayers and plasma membranes of mammalian cells. *Annu. Rev. Biophys. Biophys. Chem.* **14**, 361–386
23. Ahmed, S.N., Brown, D.A., and London, E. (1997) On the origin of sphingolipid/cholesterol-rich detergent-insoluble cell membranes, physiological concentrations of cholesterol and sphingolipid induce formation of a detergent-insoluble, liquid-ordered lipid phase in model Membranes. *Biochemistry* **36**, 10944–10953
24. Mehlhorn, I.E., Florio, E., Barber, K.R., Lordo, C., and Grant, C.W.M. (1988) Evidence that trans-bilayer interdigitation of glycosphingolipid long chain fatty acids may be a general phenomenon. *Biochim. Biophys. Acta* **939**, 151–159
25. Yohe, H.C., Roark, D.E., and Rosenberg, A. (1976) C20-sphingosine as a determining factor in aggregation of gangliosides. *J. Biol. Chem.* **251**, 7083–7087
26. Ramstedt, B., Leppimaki, P., Axberg, M., and Slotte, P.J. (1999) Analysis of natural and synthetic sphingomyelins using high-performance thin-layer chromatography. *Eur. J. Biochem.* **266**, 997–1002
27. Sonnino, S., Cantu, L., Corti, M., Acquotti, D., and Venerando, B. (1994) Aggregative properties of gangliosides in solution. *Chem. Phys. Lipids* **71**, 21–45
28. Brocca, P. and Sonnino, S. (1997) Dynamic and spatial organization of surface gangliosides. *Trends Glycosci. Glycotechnol.* **9**, 433–445
29. Pincelli, M.M., Levstein, P.R., Fidelio, G.D., and Gennaro, A.M. (2000) Cholesterol-induced alterations of the packing properties of gangliosides, an EPR study. *Chem. Phys. Lipids* **104**, 193–206
30. Schnitzer, J.E. (2001) Caveolae, from basic trafficking mechanisms to targeting transcytosis for tissue-specific drug and gene delivery *in vivo*. *Adv. Drug Deliver. Rev.* **49**, 265–280